Quantifying Uncertainty in Multiscale Heat Conduction Calculations

Prabhakar Marepalli
School of Mechanical Engineering,
The University of Texas at Austin,
Austin, TX 78712-0292
e-mail: pmarepalli@utexas.edu

Jayathi Y. Murthy[1]
School of Mechanical Engineering,
The University of Texas at Austin,
Austin, TX 78712-0292
e-mail: jmurthy@me.utexas.edu

Bo Qiu
Department of Mechanical Engineering,
Massachusetts Institute of Technology,
Boston, MA 02139
e-mail: qiub@mit.edu

Xiulin Ruan
School of Mechanical Engineering,
Purdue University,
West Lafayette, IN 47907
e-mail: ruan@purdue.edu

In recent years, there has been interest in employing atomistic computations to inform macroscale thermal transport analyses. In heat conduction simulations in semiconductors and dielectrics, for example, classical molecular dynamics (MD) is used to compute phonon relaxation times, from which material thermal conductivity may be inferred and used at the macroscale. A drawback of this method is the noise associated with MD simulation (here after referred to as MD noise), which is generated due to the possibility of multiple initial configurations corresponding to the same system temperature. When MD is used to compute phonon relaxation times, the spread may be as high as 20%. In this work, we propose a method to quantify the uncertainty in thermal conductivity computations due to MD noise, and its effect on the computation of the temperature distribution in heat conduction simulations. Bayesian inference is used to construct a probabilistic surrogate model for thermal conductivity as a function of temperature, accounting for the statistical spread in MD relaxation times. The surrogate model is used in probabilistic computations of the temperature field in macroscale Fourier conduction simulations. These simulations yield probability density functions (PDFs) of the spatial temperature distribution resulting from the PDFs of thermal conductivity. To allay the cost of probabilistic computations, a stochastic collocation technique based on generalized polynomial chaos (gPC) is used to construct a response surface for the variation of temperature (at each physical location in the domain) as a function of the random variables in the thermal conductivity model. Results are presented for the spatial variation of the probability density function of temperature as a function of spatial location in a typical heat conduction problem to establish the viability of the method. [DOI: 10.1115/1.4027348]

Keywords: uncertainty quantification, heat transfer, multiscale modeling, computational fluid dynamics

1 Introduction

Multiscale simulations are increasingly the norm in a variety of heat transfer applications. In thermal analysis of microelectronics, for example, phonon relaxation times used in transistor heat transfer calculations are computed using molecular dynamics simulations [1–8]. In the analysis of multimaterial thermal transport problems, interface transmissivity and reflectivity may be computed from atomistic simulations [9]. Increasingly there is interest in coupling molecular dynamics to flow or thermal transport simulations [10–12] to resolve near-wall subcontinuum physics. In many of these cases, deterministic macroscale simulations must be coupled to noisy molecular dynamics simulations (MD), from which effective properties are computed for use at the macroscale. The noise in MD simulations arises from the fact that the atoms in a given MD setup can have several possible initial velocity configurations all of which satisfy the constraint of total energy defined by the system temperature and the condition that there is no overall momentum. Thus, macroscale parameters such as thermal conductivity, computed from multiple realizations of the initial atomic positions and velocities, have a spread in values, or MD noise. The question we seek to answer is: What is the effect of MD noise on macroscale predictions?

The particular focus of this paper is the computation of phonon relaxation times in semiconductors and dielectrics, and the use of these relaxation times in computing thermal conductivity for use in macroscale thermal transport computations. Over the last decade, there has been a spate of simulation techniques published for submicron thermal transport based on the Boltzmann transport equation, typically under the relaxation time approximation [13–21]. Though many of these papers employ approximate relaxation times obtained from fitting experimentally-measured thermal conductivities [22,23], there have been efforts to obtain relaxation times in a more rigorous manner, either by employing perturbation theory [24–30] or through molecular dynamics [1–8].

MD simulation solves the classical multibody dynamics problem to compute the trajectory of each atom in the system at a given temperature. The interactions between the atoms are typically modeled using empirical interatomic potentials, which are readily available for many materials. The computed trajectories are then post processed using techniques from statistical mechanics to extract thermal properties such as phonon relaxation times, mean free paths, phonon dispersion, bulk thermal conductivity, and the like. These post processing techniques use lattice dynamics to extract phonon properties from MD simulations. For example, McGaughey and Kaviany [20] decomposed the total energy of the system (potential and kinetic) into its normal modes, where each mode is specified by its wave-vector and polarization. This information is then used to compute the autocorrelation function of the energy of each of these modes. The time-constant of the temporal decay of the autocorrelation function provides the relaxation time of a given mode. Henry and Chen [7] used a slightly different approach by computing the time history of the amplitudes of the normal mode instead of energy. The decay constant of this amplitude provides the relaxation time of a given mode. Another approach was developed by Thomas et al. [5,6] where they computed the spectral energy density (SED) of the system as

[1]Corresponding author.

Contributed by the Heat Transfer Division of ASME for publication in the Journal of Heat Transfer. Manuscript received April 7, 2013; final manuscript received March 29, 2014; published online August 26, 2014. Assoc. Editor: Robert D. Tzou.

a function of phonon wave-vector and frequency. When plotted against frequency spectrum, the SED displays peaks at the corresponding phonon frequencies. Furthermore, these peaks assume a Lorentzian shape, the half-width of which is used to compute the phonon relaxation time. In all the above methods, once the relaxation times are obtained, the thermal conductivity is computed using kinetic theory [2]. The reported values of thermal conductivity computed using the above procedures has an uncertainty of around 20–60 W/mK, which may be as high as 40% of the mean value.

This observed variation in phonon relaxation times results from the fact that the atomic velocities in MD simulations at a given temperature can be initialized with different configurations, with each configuration providing a different trajectory of atoms. In a typical MD calculation, a random number corresponding to a given distribution (say, Gaussian) is used to initialize atomic velocities. Several initialization configurations are obtained for a given temperature by sampling this random number. MD simulations are then performed with each of these initializations and the average of all the results is used as the representative value at that temperature.

Although the above method is widely used, the use of average values ignores the spread in relaxation times, and indeed, their statistical distribution. Depending on the nonlinearity of the macroscale problem, this spread may be manifested in a significant and spatially-variable spread in the computed temperature profiles. Indeed, this spread may far exceed the error bands engendered by numerical error, and accounting for it may be essential for making comparisons with macroscale experimental measurements.

Over the last decade, there has been significant interest in uncertainty quantification (UQ) in engineering simulations [31–33]. The focus has been on developing verification and validation protocols, and more recently, on integrating aleatoric uncertainties (due to natural variability in simulation inputs), epistemic or model form uncertainties (i.e., lack of knowledge about the physics), and experimental and numerical errors, in order to derive PDFs of simulation predictions. From these, the user may draw rigorous conclusions about the probability of specific simulation output metrics being achieved.

Bayes networks have emerged as a useful framework within which to combine calibration [34], validation, and uncertainty quantification [35–38]. Though Bayesian inference techniques have long been a staple of the reliability literature [34,38,39], application of Bayesian uncertainty quantification to microscale and multiscale systems is relatively new. A recent work in quantifying the uncertainty in multiscale fluid flow simulations is that by Salloum et al. [40], demonstrated on a Couette flow problem. They used MD to model the atomistic behavior of a thin layer of fluid close to the stationary wall and continuum modeling for the rest of the domain. The velocity of the fluid layer at the interface between atomistic and continuum domain was used to communicate between these two scales. gPC expansions of fluid velocities at the interface of the scales were constructed, with MD noise as one of the random variables. These polynomials were used to propagate uncertainty from the atomistic to macroscale and then back to atomistic scale until their coefficients converged. They used Bayesian inference to construct a surrogate model that could replace computationally expensive MD. Similar techniques are used by these authors to quantify the uncertainty in MD simulations of concentration driven ionic flow through nanopores [41,42]. To our knowledge, these approaches have never been used in multiscale heat transfer computations.

Another important set of tools for uncertainty quantification are the class of surrogate models. Traditional Monte Carlo approaches [43] for uncertainty propagation sample different realizations from the space of random parameters (input values, system properties, etc.) governing the problem and evaluate the solution of the deterministic computational model for each of these realizations. The process generates the PDF of the output quantity of interest (QoI) as a function of input PDFs. Although sampling forms the mainstay of UQ, it is prohibitively expensive when the computational model is expensive. A variety of surrogate modeling methods have been developed to allay cost. These techniques use the solution of the computational model at a selected number of test points in the random parameter space to generate a surrogate model that is computationally inexpensive but can capture the behavior of exact model to an acceptable degree. The number of test points used for surrogate models is usually substantially lower than that required for sampling approaches.

Popular methods for surrogate models include Gaussian process models and gPC expansions [44], among others. In Gaussian process models [45], the output QoI is expressed as a Gaussian with a mean and covariance function. The form of mean and covariance are determined by the type of available data and the required level of flexibility in the surrogate model. Typically, the mean of the distribution is given a functional form derived from the data or sometimes simply set to zero. If there is noise in the test data, it can be accounted for by adding an extra covariance to the mean. The magnitude of this covariance function is determined by the magnitude of noise in the data. Similarly, the covariance function of a Gaussian process is computed based on the type of available data. One of the advantages of Gaussian process models is that the mean and covariance functions need not be constrained by any assumptions about functional form. Instead they allow the data to determine these forms by introducing hyperparameters. Using the principle of maximum marginal likelihood, Gaussian process models compute the values of these hyperparameters based on the available test data. Once computed, these hyperparameters, can be used to generate the distribution of data at an unknown input location.

The gPC approach has recently gained popularity in engineering applications [46–49] as a way of representing the stochastic relationship between the inputs and outputs of a model. In this method the output QoI is expressed as an expansion in orthogonal basis polynomials that are functions of random parameters of the system. Ghanem and Spanos [50] first proposed the stochastic Galerkin method using a Weiner-Hermite polynomial chaos expansion to address Gaussian random variables. This was later generalized by Xiu and Karniadakis [46–49] to address other distributions using the Weiner-Askey scheme. Stochastic Galerkin schemes derive a new system of coupled equations for the expansion coefficients, which are then solved deterministically. A disadvantage of this method is that it is intrusive and the new system of equations may not always have an easy deterministic solution. More recently, nonintrusive stochastic collocation techniques have gained in popularity [49,51]. Here, the original system of equations is solved deterministically, but only at selected collocation points, typically sparsely distributed [52] in the multidimensional random parameter space. These collocation points are then used in interpolation schemes to reconstruct the coefficients of the polynomial expansion [49–53]. Recently, adaptive stochastic collocation schemes have begun to appear in which the sparse grid is constructed adaptively based on the error distribution [54,55].

In this paper, we present a method to propagate the uncertainty in phonon relaxation rates resulting from MD noise to compute its effect on the macroscale temperature distribution for heat conduction in bulk silicon. We use Bayesian inference to construct a probabilistic model for bulk silicon thermal conductivity using MD simulations of phonon relaxation times. A generalized polynomial chaos expansion of the temperature field in the silicon heat conduction problem is constructed in terms of the random variables in the thermal conductivity model. This gPC surrogate model is then used to compute the PDF of the two-dimensional temperature distribution subject to the noise in the thermal conductivity resulting from MD noise.

In the sections that follow, we discuss the main components of our procedure viz. (i) extraction of phonon relaxation times and thermal conductivity from MD simulations, (ii) the Bayesian inference method to construct a probabilistic surrogate thermal conductivity model from thermal conductivity data, (iii) a deterministic solution procedure for the 2D Fourier heat conduction equation,

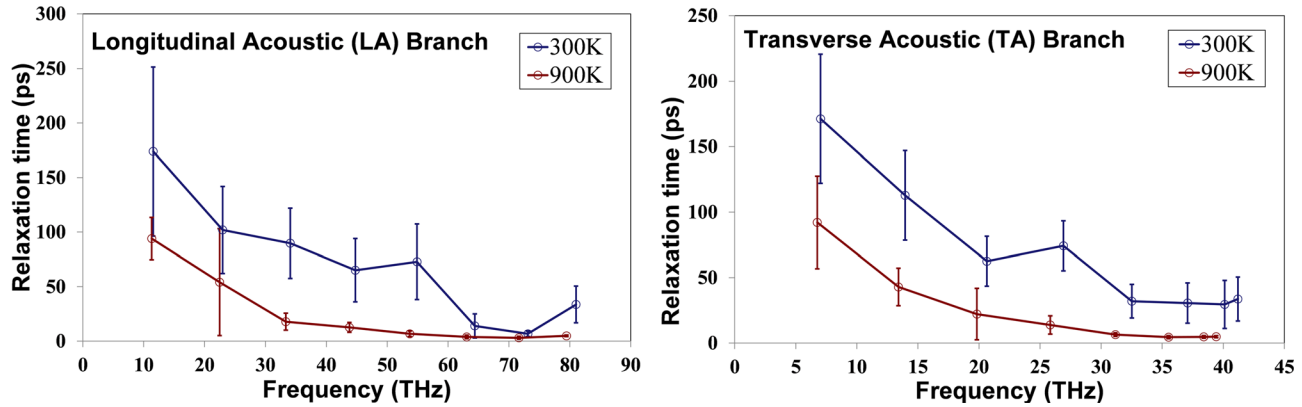

Fig. 1 Phonon relaxation times for LA and TA branches at 300 K and 900 K

and finally (iv) the procedure to quantify the uncertainty in the macroscale temperature distribution due to MD noise. Finally, we present verification results for our method, and demonstrate its use in the probabilistic computation of thermal transport in silicon.

2 Phonon Relaxation Time Computations Using Molecular Dynamics

The starting point in the computation procedure is the determination of phonon relaxation times using molecular dynamics (MD) simulation. A periodic domain containing silicon atoms is simulated, using the Stillinger-Weber potential [56] using the LAMMPS solver [57]. A total number of 4096 atoms ($\xi = 8$, where ξ is number of unit cells in each atomic direction corresponding to total number of $8\xi^3$ atoms) are used for the simulation. Size effects due to the finite domain size have been examined in Ref. [58]. In Ref. [59], it was shown that thermal conductivity calculations became size independent beyond about 216 atoms, albeit using the environment-dependent interatomic potential. Therefore, thermal conductivity computations performed here with 4096 atoms are expected to be domain-independent. All simulations used a lattice constant of 0.56309 nm and a time step of 1 femtosecond. Each simulation involves 4.4×10^6 time steps from which 2×10^5 steps correspond to pressure equilibration using an NPT (i.e., constant number of atoms, pressure, and temperature) ensemble and 2×10^5 steps correspond to energy equilibration using an NVE (i.e., constant number of atoms, volume, and energy) ensemble [60]. The simulations are performed at seven different temperatures (300 K–900 K) with 20 realizations at each temperature. At a given temperature, each realization has different initial atomic velocity obtained by changing the random seed of the Gaussian distribution that controls the velocity initialization. Atomic velocities are collected every 10 time steps for post processing.

In order to compute the lattice thermal conductivity of silicon as a function of temperature, we examine the spectral properties of individual phonon modes through the spectral energy density (SED) analysis discussed in Ref. [5]. The advantage of the SED method is that it does not require any adjustable parameters and can be readily integrated with MD simulations to extract the fully-anharmonic phonon frequencies and associated phonon scattering rates for individual modes.

In this method, the SED function may be derived as

$$\psi(\mathbf{k},\omega) = \sum_{\alpha}^{3}\sum_{b}^{n_b}\frac{m_b}{4\pi\tau_0 N_T}\left|\int_0^{\tau_0}\sum_{l}^{N_T}\dot{u}_{\alpha}^{b,l}(t)\times\exp[i\mathbf{k}.\mathbf{r}_0^l - i\omega t]dt\right|^2 \tag{1}$$

where $\mathbf{k}$ is the wave vector, ω is the angular frequency, τ_0 is the integration time constant (1 ns in this work), α represents the x, y, z coordinate directions, b is the index of basis atoms, and n_b is the number of basis atoms in the chosen cell. Furthermore, l is the index of cells, N_T is the total number of cells in the MD domain, and m_b is the atomic mass of the basis atom b. Also, $\dot{u}_{\alpha}^{b,l}$ (t) is the α component of the velocity of basis atom b in cell l and $\mathbf{r}_0^l$ is the equilibrium position of cell l. It can be shown that the SED function is a linear superposition of $3n$ Lorentzian functions with centers at the fully-anharmonic phonon frequency $\omega_0(k, v)$

$$\psi(\mathbf{k},\omega) = \sum_{v}^{3n_b}\frac{C(\mathbf{k},v)}{[2\tau(\omega-\omega_0(\mathbf{k},v))]^2+1} \tag{2}$$

where v is the index of phonon branches and $C(\mathbf{k}, v)$ is the combination of coefficients as weighting factors for Lorentzian functions. τ is the fully-anharmonic phonon relaxation time. By constructing the SED function based on Eq. (1) using the atomic velocities from MD simulations and fitting Eq. (2) to it, ω_0 and τ can be extracted for a given $\mathbf{k}$.

Using the above procedure, the phonon dispersion relation, i.e., the ω versus $\mathbf{k}$ relation, and the relaxation times as a function of wave vector $\mathbf{k}$ (or frequency ω) are obtained for each phonon branch. For silicon, with 2 atoms per unit cell, and 3 coordinate directions x, y, z, we obtain a total of 6 phonon branches. Three of these are acoustic branches (longitudinal acoustic (LA) and two transverse acoustic (TA)) and the other three are optical branches (longitudinal optical and two transverse optical). In order to capture the behavior of phonons accurately in the entire wave vector space, the dispersion relation must be computed in the volume of the entire first Brillouin zone. To allay cost, for a material like silicon, it is customary to restrict computations to high-symmetry directions such as [100], [010], [001] and further, under assumptions of isotropy, to pick one of these directions as representative of the entire Brillouin zone. For this paper, we obtain properties in [100] direction and make an isotropic assumption to compute macroscopic parameters. This assumption means that the first Brillouin zone is spherical in shape and the phonon properties are same along all the directions. This assumption is reasonably good for silicon and has been used in several past computations, Ref. [7] for example.

In Fig. 1, we show the relaxation times for LA and TA phonon branches at 300 K and 900 K computed using the procedure described above, with error bars due to MD noise. The variation in error bars at different frequencies is due to the nonlinear nature of the interatomic potential used for MD simulations. The error bars represent the upper/lower bound of relaxation time from the 20 samples simulated.

Once the relaxation times (τ_r) and dispersion relations are obtained for all phonon branches, the thermal conductivity for each MD realization may be obtained under the assumption of Brillouin zone isotropy as [2]

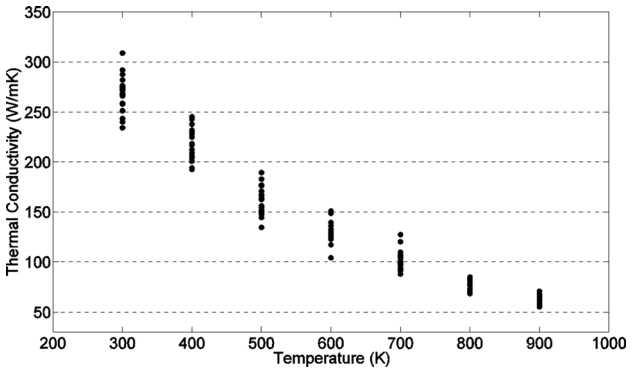

Fig. 2 Thermal conductivity of silicon at different temperatures. The scatter in the data at each temperature is due to MD noise.

$$k = \frac{4\pi}{3}\frac{1}{(2\pi)^3}\sum_{\text{polarization}}\int_0^{w_{\max}}\left(c_v\frac{v_g}{v_p^2}\tau_r\right)\omega^2 d\omega \tag{3}$$

In this equation, ω is the phonon frequency, τ_r is the relaxation time, v_g is group velocity given as $v_g = (\partial\omega/\partial\boldsymbol{k})$, v_p is the phase velocity given as $v_p = \omega/\kappa$. The phonon specific heat c_v is taken as $c_v = (\partial/\partial T)\hbar\omega f^0$.

As mentioned above, twenty independent simulations are performed with different velocity initializations to obtain the scatter in thermal conductivity at a given temperature. The same procedure is then repeated for different temperatures to get the scatter at all required temperatures. At any given temperature, there is a scatter in the τ_r values obtained from MD, resulting in a scatter in the thermal conductivity. In Fig. 2, we show the computed thermal conductivity at different temperatures with the associated scatter. While there are other sources of uncertainty in this simulation such as domain size and time-step size, the procedures for accounting for these are well-established. Consequently, in this paper, we focus on the effect of MD noise in macroscale simulations. This choice is justified by the fact that even with all the other numerical/simulation parameters fixed we observe a noise of about 20% solely due to random initializations, clearly demonstrating the magnitude of this effect. This magnitude is far larger than the error in thermal conductivity due to domain size or time-step effects.

3 Bayesian Inference: Surrogate Model for Thermal Conductivity

As mentioned earlier, computation of thermal conductivity from MD simulation is computationally quite expensive. Furthermore, it is important to capture the dependence of thermal conductivity on temperature in many problems of technological interest. In order to allay MD cost, we construct a surrogate model for conductivity using the available MD simulation data at selected temperatures. We choose a surrogate model of the form

$$k = v_0 T^{v_1} + v_2 + (v_3 T + v_4)\eta, \quad \eta \overset{i.i.d}{\sim} N(0,1) \tag{4}$$

where $v_0 T^{v_1} + v_2$ is the mean and $v_3 T + v_4$ is the standard deviation; a normal distribution is assumed. The assumption of normal distribution is made only for the sake of simplicity; the same procedure can be directly applied to any type of distribution. The coefficients, v_0, v_1, v_2 are obtained by fitting the mean of the thermal conductivity data to the expression $v_0 T^{v_1} + v_2$. The coefficients v_3 and v_4 are chosen to be random parameters, the distribution of which is obtained by calibrating the functional form of k to the (noisy) values of thermal conductivity data obtained from MD. Bayesian inference is used to perform the calibration. This procedure is similar to that used by Salloum et al. in Refs. [40–42]. The advantage of Bayesian inference is that the calibrated coefficients take the form of a PDF instead of deterministic values. The PDFs allow the surrogate models to capture not only the temperature dependence of conductivity but also the MD noise at each temperature.

The Bayesian inference procedure is now outlined. Assuming an inverse power variation of thermal conductivity with temperature ($k = v_0 T^{v_1} + v_2$, where v_0, v_1, v_2 are deterministic and v_1 is typically negative), and the noise in thermal conductivity as a linear function of temperature ($\sigma = v_3 T + v_4$), we may calibrate the coefficients v_3 and v_4 using Bayes' theorem as

$$\Pr(v_3, v_4|k_{\text{MD}}) = \frac{\Pr(k_{\text{MD}}|v_3, v_4)\pi(v_3)\pi(v_4)}{\iint \Pr(k_{\text{MD}}|v_3, v_4)\pi(v_3)\pi(v_4)\mathrm{d}v_3\mathrm{d}v_4} \tag{5}$$

where the left hand side of Eq. (5) is called the *joint posterior probability*, k_{MD} are the available conductivity data from MD simulations; $\Pr(k_{\text{MD}}|v_3, v_4)$ is called the joint likelihood, and denotes the probability that the conductivity k_{MD} is observed for the given values of v_3, v_4; $\pi(v_3), \pi(v_4)$ are the prior values (or initial guesses) of these coefficients; and the denominator is the total probability, a normalizing constant. The joint likelihood function is given as

$$\begin{aligned} &\Pr(k_{\text{MD}}|v_3, v_4) = \pi(k_{\text{MD}}|k) \\ &k_{\text{MD}} = k + (v_3 T + v_4)\eta, \quad \eta \overset{i.i.d}{\sim} N(0,1) \\ &k = v_0 T^{v_1} + v_2 \\ &\pi(k_{\text{MD}}|k) = N(v_0 T^{v_1} + v_2, (v_3 T + v_4)^2) \end{aligned} \tag{6}$$

Once the likelihood is computed using Eq. (6), Markov chain Monte Carlo sampling using the Metropolis-Hastings algorithm [39] is used to sample values of v_3 and v_4 from the joint likelihood function $\Pr(k_{\text{MD}}|v_3, v_4)$ and a PDF is constructed from these values using a kernel density estimator.

The PDFs of v_3 and v_4 so obtained are shown in Figs. 3(*a*) and 3(*b*). In order to check how well the surrogate model of Eq. (4) can reproduce the noise in the thermal conductivity distribution, we sample the values of v_3 and v_4 and substitute them in Eq. (4) to obtain corresponding thermal conductivity data. Also, by fitting the mean values of MD data to the expression $k = v_0 T^{v_1} + v_2$, the coefficients v_0, v_1, v_2 are obtained as $v_0 = 3.7288 \times 10^3\,\text{W/mK}^{v_1+1}$, $v_1 = -0.2548$, and $v_2 = -600.2143\,\text{W/mK}$. This data are plotted on the top of the actual thermal conductivity data in Fig. 3(*c*) and we can clearly see from the figure that the surrogate model captures the MD noise reasonably well.

3.1 Assessment of Surrogate Model.

Here we discuss the methodology to assess the goodness-of-fit of the surrogate model constructed in the above section. We use the method of Bayesian hypothesis testing discussed in Ref. [36,38] to introduce a metric called the Bayes factor that can quantify the accuracy of the model. We define the Bayes factor as the ratio of likelihoods of two hypotheses or models (H_0 and H_1).

$$B = \frac{P(D|H_0)}{P(D|H_1)} \tag{7}$$

where H_0 refers to the model calibrated using Bayesian inference, H_1 refers to the actual model which is used as standard for comparison, and D is the data used to assess goodness-of-fit. In other words, the Bayes factor quantifies the accuracy with which the surrogate model captures the actual model. In our case, the form of hypothesis H_1, i.e., the actual model, is not readily available. Therefore, we assume the model H_1 to be uniform distribution,

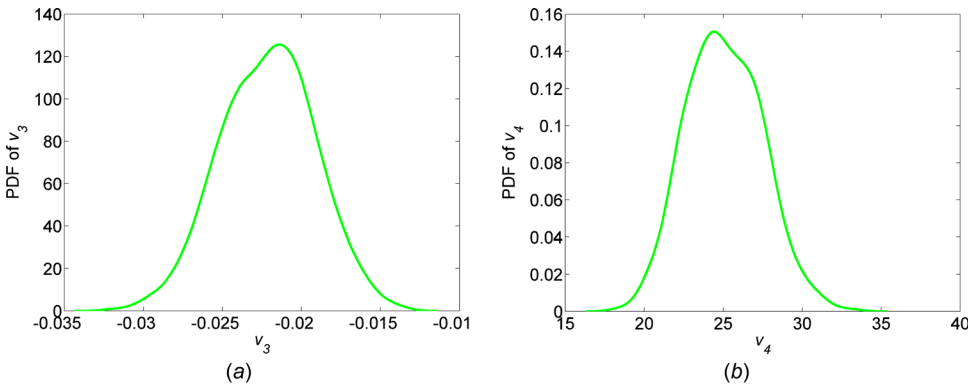

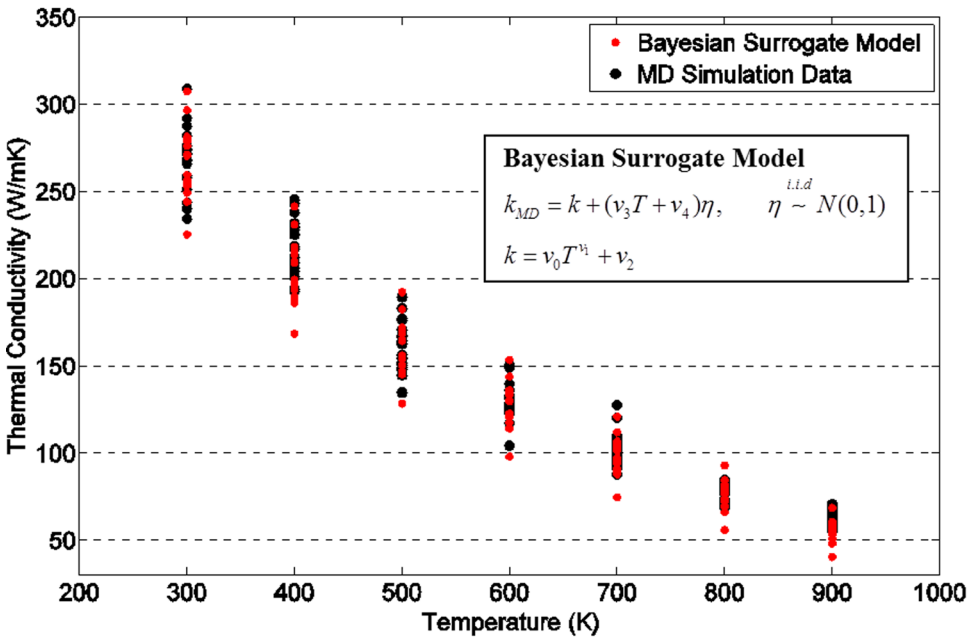

Fig. 3 (*a*) and (*b*) Calibrated coefficients in the functional form of thermal conductivity surrogate model. (*c*) Thermal conductivity data reproduced by surrogate model. Data points in black represent the MD simulation data and the data points in red are those generated using surrogate model. The surrogate model captures the temperature dependence and the MD noise of thermal conductivity well.

Table 1 Overall Bayes factors for real MD data

Temperature (K)	Overall Bayes factor
300	$6.01678 \times 10^{+22}$
400	$1.75586 \times 10^{+22}$
500	$4.04599 \times 10^{+24}$
600	$2.65532 \times 10^{+27}$
700	$1.8649 \times 10^{+28}$
800	$1.80037 \times 10^{+32}$
900	$3.92568 \times 10^{+32}$

consistent with the fact that no information is available about the actual model.

In the case of multiple data points D_i for assessment, where $i = 1$ to N, with N being the number of data points, and given that the data points are independent of each other, the overall Bayes factor is equal to the product of Bayes factors computed for individual data points given by

$$B = \frac{P(D_1|H_0)P(D_2|H_0).....P(D_N|H_0)}{P(D_1|H_1)P(D_2|H_1).....P(D_N|H_1)} = B_1B_2.....B_N \quad (8)$$

The individual value B_i corresponding to data point i is computed as

$$B_i = \frac{\iint_{v_3,v_4} \pi_0(k_D^i|v_3,v_4)\pi(v_3,v_4)dv_3dv_4}{\pi(k_D^i|k_{\text{actual}})}$$
$$\pi_0 \sim N(v_0T^{v_1} + v_2, (v_3T + v_4)^2)$$
where v_3 and v_4 are calibration coefficients
$$\pi \sim \text{Uniform distribution} \quad (9)$$

A Bayes factor greater than 1 suggests that the surrogate model is better than a model with a uniform distribution. In Table 1, we show the overall Bayes factors using the real MD data for temperatures between 300 and 900 K. Also, the individual Bayes factors (B_1, B_2,..., B_N) are observed to be in range between 1.3 and 84, i.e., greater than unity.

4 Numerical Method

For the purposes of demonstration, steady Fourier heat conduction is considered, with a random thermal conductivity such as that resulting from MD simulations. The finite volume method

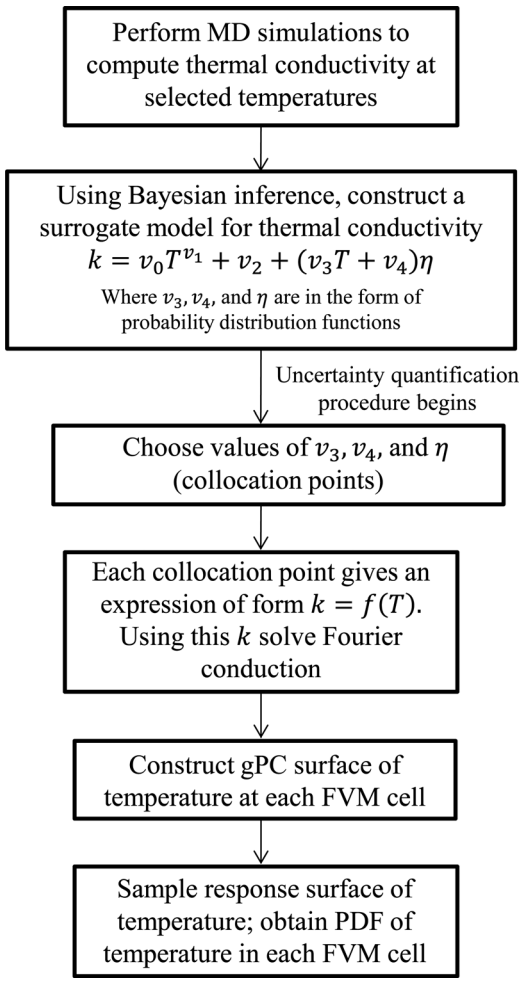

Fig. 4 Solution procedure to quantify uncertainty in multiscale heat conduction problem

[61] is used to discretize the deterministic energy equation. A spatially second-order accurate scheme is employed. The resulting set of nominally linear algebraic equations is solved using line-by-line tridiagonal matrix algorithm [61].

5 Uncertainty Quantification

In this section, we describe our approach to account for the MD noise in the thermal conductivity and propagate it to the continuum scale to quantify its effect on the predicted temperature profile. The objective is to generate a PDF of temperature distribution in the physical domain resulting from the PDF of thermal conductivity. This resulting PDF may be used to assess confidence in temperature predictions, where a PDF with the smaller standard deviation implies greater confidence.

The standard procedure to achieve this is to generate samples of random parameters that govern the conductivity (see Eq. (4)), and solve the Fourier equation numerically using the conductivity computed from each of these samples. There are various procedures to generate random samples, including Monte Carlo (MC) sampling, latin hypercube sampling (LHS), etc., with MC being the gold standard. Each realization of these samples yields a field of temperature, $T(x,y)$. If the sample size is sufficiently large, the PDF of temperature constructed from these solutions represents the actual distribution of temperature due to MD noise. However, the above procedure is computationally very expensive when there is large number of random parameters and when the deterministic finite volume solution is computationally-intensive. An alternate and more efficient approach is to construct a gPC response surface of temperature with the coefficients of thermal

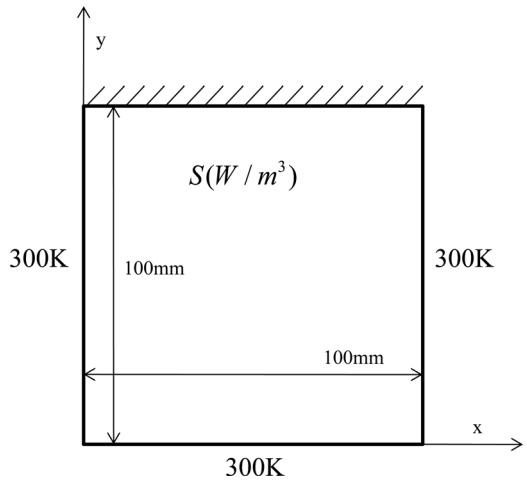

Fig. 5 Schematic and boundary conditions

conductivity surrogate model (v_3, v_4, and η) as the random variables of expansion. This approach generates collocation points at which the deterministic solution $T(x,y)$ of Fourier equation is required. The number of collocation points required for gPC is significantly lower than the number of Monte Carlo samples typically needed. In this work, we use Smolyak sparse grid algorithm [52] to generate the collocation points and the response surface is constructed using the Purdue UQ (PUQ) software from Purdue University [62].

Given the surrogate model for thermal conductivity $k = v_0 T^{v_1} + v_2 + (v_3 T + v_4)\eta$, where v_3 and v_4 are the calibrated PDFs, the solution procedure is as described below (see Fig. 4).

(1) Choose a set of N collocation points for v_3, v_4, and η.
(2) Substitute the above points in Eq. (4) to obtain the corresponding points in thermal conductivity space.
(3) Using the finite volume method on the discretized domain, solve the Fourier equation at all the collocation points. This step provides N temperature solutions $T(x,y)$ that correspond to N collocation points.
(4) Using these solutions, construct a gPC response surface for temperature at each finite volume cell.
(5) Sample the gPC response surface and construct a PDF of temperature at each cell.

6 Results

In this section, we present the results of our methodology followed by a discussion of our findings.

6.1 Problem Description. We consider the problem of heat conduction in a square domain, as shown in Fig. 5. A square domain of side 100 mm is considered. The Fourier conduction equation solved in the physical domain is given by

$$\nabla.(k\nabla T) + S = 0 \tag{10}$$

where T is the temperature, k is the thermal conductivity given by Eq. (4), and S is the source term. We use a nonlinear source term of the form $S = AT^3(T_\infty - T)$ where $T_\infty = 800$ K. Several cases of the above problem are examined and the value of A is chosen in order to suit each of those cases, as described in the Sec. 6. The domain is discretized into a uniform rectangular mesh of 20×20. Discrete values of T and the thermal conductivity k are stored at cell centroids.

6.2 Uncertainty Quantification

6.2.1 Effect of Nonlinearity in Thermal Conductivity. We first investigate the effect of nonlinearity in the PDF of thermal conductivity on the temperature distribution. For this we synthetically

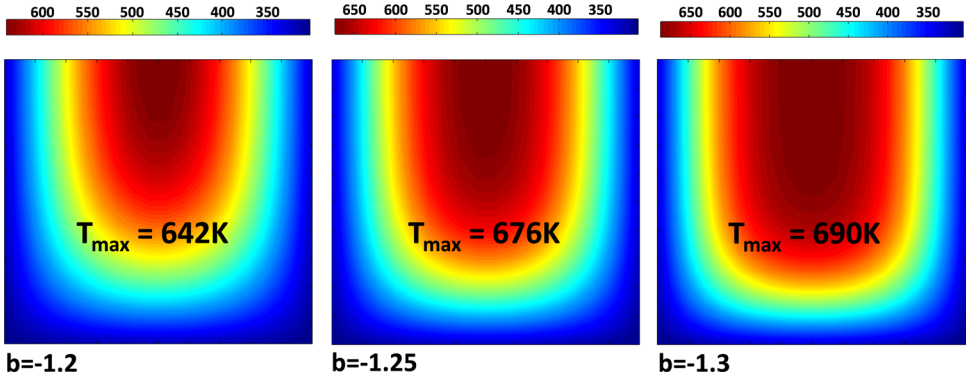

Fig. 6 Mean temperature contours for different orders of nonlinearity in thermal conductivity ($k = aT^b + \sigma\eta$)

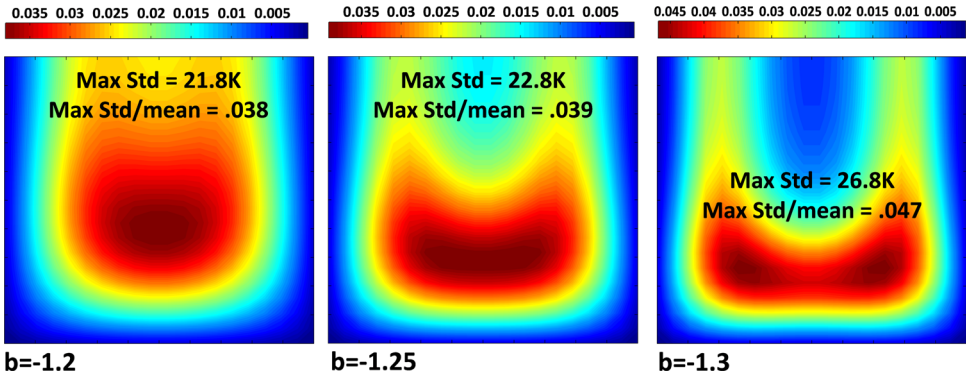

Fig. 7 Ratio of standard deviation to mean temperature for different orders of nonlinearity in thermal conductivity ($k = aT^b + \sigma\eta$)

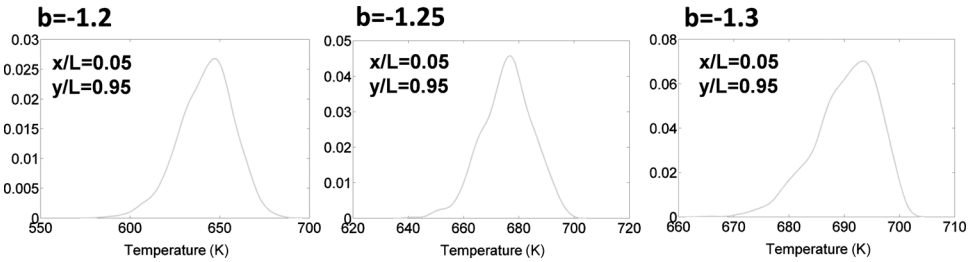

Fig. 8 PDF of temperature at a given spatial location for different degrees of nonlinearity in the temperature dependence of thermal conductivity

generate three simple test cases of thermal conductivity data with each case having different orders of nonlinearity. The data are generated using the conductivity relation of the form

$$k = aT^b + \sigma\eta, \quad \eta \sim N(0,1)$$

where $a, b,$ and σ are deterministic coefficients with the nonlinearity in thermal conductivity governed by the inverse power of temperature b. Three different cases with $b = -1.2$, $b = -1.25$, and $b = -1.3$, respectively, are considered. The values of a and σ for all three cases are $2.5 \times 10^5\ \mathrm{W/mK}^{b+1}$ and $15\ \mathrm{W/mK}$, respectively. By fixing the coefficients $a, b,$ and σ to be deterministic, the only source of uncertainty in thermal conductivity is through η, which is chosen to have a normal distribution of mean 0 and standard deviation of 1.

As described earlier, the uncertainty in temperature distribution is obtained by constructing a gPC response surface of temperature as a function of random variables, which in this case is just η, i.e., $T(x,y) = f(x,y,\eta)$. A fourth-order Legendre polynomial is used to generate the collocation points. A total of 17 collocation points are generated. The same Fourier problem, $\nabla.(k\nabla T) + S = 0$ with $S = AT^3(T_\infty - T)$ is solved for the three cases. The value of A used for these cases is $0.0024\ \mathrm{W/m^3K^4}$ and $T_\infty = 700\,K$.

Once the gPC response surface of temperature is obtained $T(x,y) = f(x,y,\eta)$, the mean and standard deviation of temperature across the physical domain are computed by sampling the values of η, as shown in Figs. 6 and 7. A noteworthy aspect of these three cases is the variation of standard deviation with the nonlinearity in thermal conductivity. As shown in Fig. 7, the standard deviation of temperature increases nonlinearly with the nonlinearity in thermal conductivity, as expected. Thus, the noise in thermal conductivity resulting from MD simulations is expected to be amplified nonlinearly, depending on the nonlinearity of the macroscale problem.

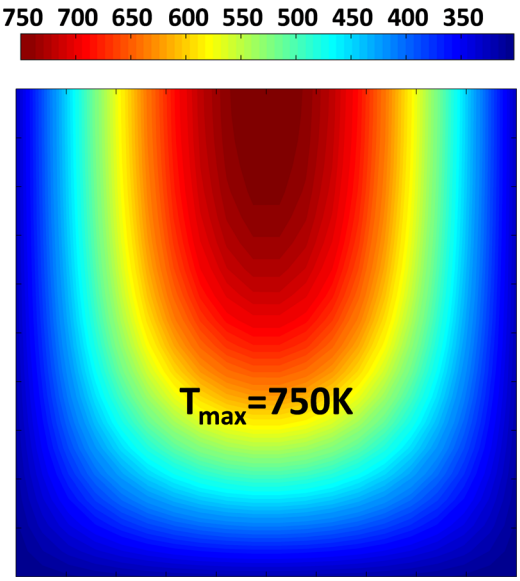

Fig. 9 Mean temperature profile (degrees K) computed by sampling the gPC response surfaces at each finite volume cell in the domain

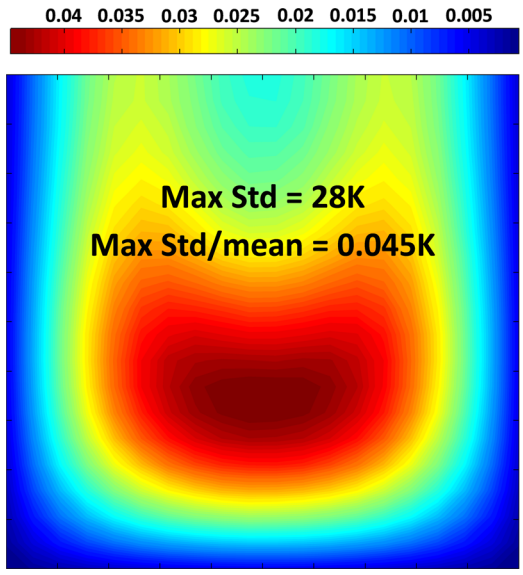

Fig. 10 Ratio of standard deviation to mean of temperature computed by sampling the gPC response surfaces at each finite volume cell in the domain

Figure 8 shows PDFs of temperature at the location $x/L = 0.05$ and $y/L = 0.95$ (considering the origin to be at the center of the domain) for different degrees of nonlinearity. This location corresponds to that of maximum temperature in the computational domain. We see that though the thermal conductivity distribution is normally distributed and thus symmetric about the mean, the resulting temperature distribution is skewed, and the degree of skewness is quite pronounced as the degree of nonlinearity in the thermal conductivity, embodied in the b factor, increases.

6.2.2 Uncertainty Quantification Using MD Data for Silicon. We now consider the propagation of uncertainty in the thermal conductivity of silicon for the heat conduction problem described above. A Bayesian surrogate for the thermal conductivity is constructed as described above. A gPC response surface of the temperature distribution is then constructed by choosing collocation points for the random parameters $v_3, v_4,$ and η in Eq. (4). We use the Smolyak sparse grid algorithm with third-order Legendre polynomials to generate these points. A total of 69 sampling points is

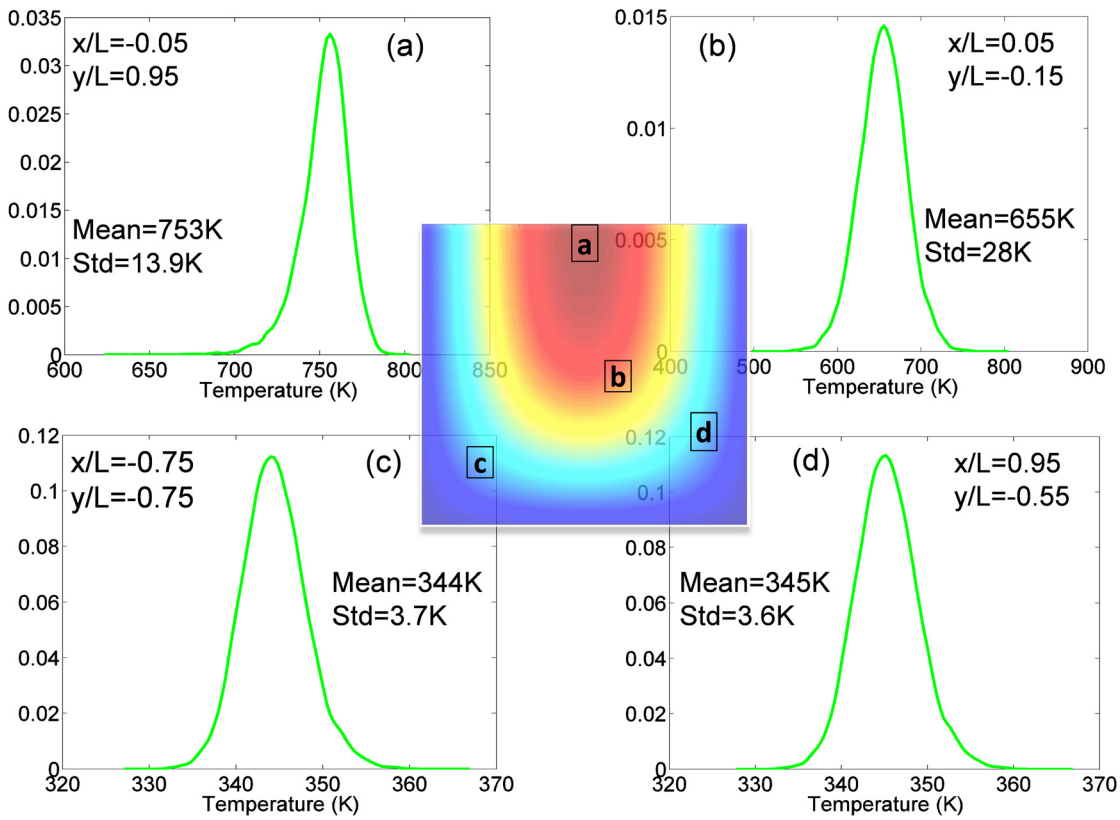

Fig. 11 PDFs of temperature at different spatial locations

generated by this algorithm. For each of the collocation points, we obtain a unique value of thermal conductivity given by $k = v_0 T^{v_1} + v_2 + (v_3^i T + v_4^i)\eta^i$ where v_3^i, v_4^i, and η^i are from a given set i of collocation points where $i = 1$–69. These values are then used to solve the deterministic Fourier problem $\nabla.(k\nabla T) + S = 0$ with $S = AT^3(T_\infty - T)$ where $A = 0.0024\,\mathrm{W/m^3K^4}$. Sixty nine different temperature solutions $T(x,y)$ are obtained. Finally, to construct a gPC response surface of temperature at each cell, we visit each finite volume cell of the discretized domain, collect the temperature data at that cell from all 69 collocation points, and use them to construct a polynomial for temperature of the form $T(x,y) = f(x,y,v_3,v_4,\eta)$. In other words, the above equation provides an inexpensive closed form polynomial relationship between the random inputs v_3, v_4, and η and the output $T(x,y)$. We employ this surrogate to directly investigate the effect of MD noise on the overall temperature distribution. Once such a polynomial is available, the PDF of temperature at each finite volume cell is generated by sampling the random parameters v_3, v_4, and η.

Using the above procedure, the contours of the mean and standard deviation of temperature are obtained as shown in Figs. 9 and 10, respectively. The maximum standard deviation is approximately 28 K, i.e., 3.7% of the maximum temperature. The corresponding standard deviation in thermal conductivity is 18.87 W/mK, 7% of the maximum value. We observe in Fig. 10 that the region of maximum standard deviation does not occur at the region of maximum temperature but at a location below the center of the domain. This behavior is due to the interplay between nonlinear thermal conductivity and nonlinear source term, and would vary from problem to problem.

The PDF of temperature at different spatial locations is shown in Fig. 11. For silicon, the nonlinearity in the temperature dependence of thermal conductivity is captured by the factor v_1 which is found to be $v_1 = -0.2548$. This relatively mild nonlinearity results in relatively symmetric temperature distributions, as seen in Fig. 11.

6.2.3 Verification Using Monte Carlo Simulation. Finally, we verify our method using standard Monte Carlo (MC) simulation for the same problem using the same thermal conductivity data. In this method, MC samples of thermal conductivity are generated by sampling the values of v_3 and v_4 from $k = v_0 T^{v_1} + v_2 + (v_3 T + v_4)\eta$. We use a total of 35,000 MC samples. The deterministic Fourier equation is then solved for each of these 35,000 thermal conductivity samples to compute the temperature profile. The mean and standard deviation computed from the above solutions is compared with corresponding mean and standard deviation obtained from gPC fit. We find good agreement between the two results, with the maximum difference between mean temperatures and standard deviations to be 0.17 K and 0.19 K respectively, i.e., 0.028% and 1.25%, respectively. This minor difference can be attributed to the accuracy with which the gPC fit can capture the uncertainty in thermal conductivity. The agreement with MC simulation results verifies the method and at the same time emphasizes the significant speed-up in the procedure: Our method requires just 69 samples to produce the same results as those obtained by 35,000 MC samples.

7 Conclusions

In this paper, we presented a method to quantify the uncertainty in thermal conductivity due to the inherent noise in MD simulations and propagate it to temperature predictions at the continuum scale. Bayesian inference is used to construct a probabilistic surrogate model for the thermal conductivity distribution as a function of temperature distribution. The effect of MD noise in thermal conductivity on the macroscale temperature is large in the areas of high temperature. This is due to the nonlinear dependence of conductivity on temperature and the presence of a nonlinear source term. Our method was verified against standard Monte Carlo simulation and showed good agreement; however, our technique was shown to be as much as three orders of magnitude less expensive than Monte Carlo simulation. The methodology developed in this paper may be generalized to compute the effect of MD noise in any problem that involves atomistic-to-continuum coupling.

Acknowledgment

We would like to thank Martin Hunt from the Rosen Center for Advanced Computing at Purdue University for help with Purdue-UQ. We would also like to thank Professor Sankaran Mahadevan, You Ling, and Shankar Sankararaman from Vanderbilt University for insightful discussions on Bayesian techniques. Support of J. Murthy from the PRISM center under DOE grant DE-FC52-08NA28617 is gratefully acknowledged. B. Qiu and X. R. Ruan acknowledge the partial support from an National Science Foundation CAREER Award (CBET-1150948).

Nomenclature

c_v = phonon specific heat $(\mathrm{J/m^3K})$
f^0 = equilibrium phonon distribution
$\hbar$ = reduced Planck's constant (Js)
k_B = Boltzmann's constant
k = material thermal conductivity
$N(0,1)$ = normal distribution with mean 0 and standard deviation 1
$\Pr(a)$ = probability that an event a occurs
$\Pr(a|b)$ = probability that an event a occurs given that event b has occurred
T = temperature (K)
UQ = uncertainty quantification
v_g = phonon group velocity (m/s)
v_p = phonon phase velocity (m/s)

Greek Symbols

Δx = length of the control volume (m)
Δy = width of the control volume (m)
$\boldsymbol{\kappa}$ = wave vector $(1/\mathrm{m})$
τ_r = relaxation times (s)
$\Phi(\boldsymbol{\kappa},\omega)$ = spectral energy density (SED) at $\boldsymbol{\kappa},\omega$
ω = frequency (rad/s)

References

[1] Goicochea, J. V., Madrid, M., and Amon, C., 2010, "Hierarchical Modeling of Heat Transfer in Silicon-Based Electronic Devices," ASME J. Heat Transfer, **132**(10), p. 102401.
[2] Goicochea, J. V., Madrid, M., and Amon, C. H., 2010, "Thermal Properties for Bulk Silicon Based on the Determination of Relaxation Times Using Molecular Dynamics," ASME J. Heat Transfer, **132**(1), p. 012401.
[3] McGaughey, A. J. H., and Kaviany, M., 2006, "Phonon Transport in Molecular Dynamics Simulations: Formulation and Thermal Conductivity Prediction," Adv. Heat Transfer, **39**, pp. 169–255.
[4] Turney, J. E., Landry, E. S., McGaughey, A. J. H., and Amon, C. H., 2009, "Predicting Phonon Properties and Thermal Conductivity From Anharmonic Lattice Dynamics Calculations and Molecular Dynamics Simulations," Phys. Rev. B, **79**, p. 064301.
[5] Thomas, J. A., Turney, J. E., Iutzi, R. M., Amon, C. H., and McGaughey, A. J. H., 2010, "Predicting Phonon Dispersion Relations and Lifetimes From the Spectral Energy Density," Phys. Rev. B, **81**(8), p. 081411.
[6] Koker, N. de., 2009, "Thermal Conductivity of MgO Periclase From Equilibrium First Principles Molecular Dynamics," Phys. Rev. Lett., **103**, p. 125902.
[7] Henry, A. S., and Chen, G., 2008, "Spectral Phonon Transport Properties of Silicon Based on Molecular Dynamics Simulations and Lattice Dynamics," J. Comput. Theor. Nanosci., **5**(2), pp. 141–152.
[8] Qiu, B., Bao, H., Zhang, G., Wu, Y., and Ruan, X., 2011, "Molecular Dynamics Simulations of Lattice Thermal Conductivity and Spectral Phonon Mean Free Path of PbTe: Bulk and Nanostructures," Comput. Mater.Sci., **53**(1), pp. 278–285.
[9] Sun, L., 2008, *Phonon Transport in Confined Structures and at Interfaces*, Ph.D. thesis, Purdue University, West Lafayette, IN.
[10] Liu, K., Chen, S., Nie, X., and Robbins, M. O., 2007, "A Continuum–Atomistic Simulation of Heat Transfer in Micro- and Nano-Flows," J. Comput. Phys., **227**(1), pp. 279–291.
[11] Werder, T., Walther, J. H., and Koumoutsakos, P., 2005, "Hybrid Atomistic–Continuum Method for the Simulation of Dense Fluid Flows," J. Comput. Phys., **205**(1), pp. 373–390.

[12] Mohamed, K. M., and Mohamad, A. A., 2010, "A Review of the Development of Hybrid Atomistic-Continuum Methods for Dense Fluids," Microfluidics Nanofluidics, **8**(3), pp. 283–302.
[13] Narumanchi, S. V. J., Murthy, J. Y., and Amon, C. H., 2004, "Submicron Heat Transport Model in Silicon Accounting for Phonon Dispersion and Polarization," ASME J. Heat Transfer, **126**(6), pp. 946–955.
[14] Narumanchi, S. V. J., Murthy, J. Y., and Amon, C. H., 2006, "Boltzmann Transport Equation-Based Thermal Modeling Approaches for Hotspots in Microelectronics," Heat Mass Transfer, **42**(6), pp. 478–491.
[15] Narumanchi, S. V. J., Murthy, J. Y., and Amon, C. H., 2005, "Comparison of Different Phonon Transport Models for Predicting Heat Conduction in Silicon-on-Insulator Transistors," ASME J. Heat Transfer, **127**(7), pp. 713–723.
[16] Ni, C., 2009, "Phonon Transport Models for Heat Conduction in Sub-Micron Geometries With Applications to Microelectronics," Ph.D. thesis, Purdue University, West Lafayette, IN.
[17] Loy, J. M., 2010, "An Acceleration Technique for the Solution of the Phonon Boltzmann Transport Equation," M.S. thesis, Purdue University, West Lafayette, IN.
[18] Majumdar, A., 1993, "Microscale Heat Conduction in Dielectric Thin Films," ASME J. Heat Transfer, **115**(7), pp. 7–16.
[19] Mazumder, S., and Majumdar, A., 2001, "Monte Carlo Study of Phonon Transport in Solid Thin Films Including Dispersion and Polarization," ASME J. Heat Transfer, **123**(4), pp. 749–759.
[20] McGaughey, A. J., and Kaviany, M., 2004, "Quantitative Validation of the Boltzmann Transport Equation Phonon Thermal Conductivity Model under the Single-Mode Relaxation Time Approximation," Phys. Rev. B, **69**(9), p. 094303.
[21] Chen, G., 1998, "Thermal-Conductivity and Ballistic-Phonon Transport in the Cross-Plane Direction of Superlattices," Phys. Rev. B, **57**(23), pp. 14958–14973.
[22] Callaway, J., 1959, "Model for Lattice Thermal Conductivity at Low Temperatures," Phys. Rev., **113**(4), pp. 1046–1051.
[23] Holland M. G., 1963, "Analysis of Lattice Thermal Conductivity," Phys. Rev., **132**(6), pp. 2461–2471.
[24] Klemens, P. G., 1951, "The Thermal Conductivity of Dielectric Solids at Low Temperatures (Theoretical)," Proc. R. Soc. A, **208**(1092), pp. 108–133.
[25] Ward, A., and Broido, D. A., 2010, "Intrinsic Phonon Relaxation Times from First-Principles Studies of the Thermal Conductivities of Si and Ge," Phys. Rev. B, **81**(8), p. 085205.
[26] Broido, D. A., Malorny, M., Birner, G., and Mingo, N., 2007, "Intrinsic Lattice Thermal Conductivity of Semiconductors From First Principles," Appl. Phys. Lett., **91**, p. 231922.
[27] Pascual-Gutiérrez, J. A., Murthy, J. Y., and Viskanta, R., 2009, "Thermal Conductivity and Phonon Transport Properties of Silicon Using Perturbation Theory and the Environment-Dependent Interatomic Potential," J. Appl. Phys., **106**, p. 063532.
[28] Pascual-Gutierrez, J. A., 2011, "On the Theory of Phonons: A Journey From Their Origins to the Intricate Mechanisms of Their Transport," Ph.D. thesis, Purdue University, West Lafayette, IN.
[29] Singh, D., Murthy, J. Y., and Fisher, T. S., 2011, "Spectral Phonon Conduction and Dominant Scattering Pathways in Graphene," J. Appl. Phys., **110**(9), p. 094312.
[30] Singh, D., 2011, "Frequency and Polarization Resolved Phonon Transport in Carbon and Silicon Nanostructures," Ph.D. thesis, Purdue University, West Lafayette, IN.
[31] Pilch, M., Trucano, T., and Helton, J., 2011, "Ideas Underlying Quantification of Margins and Uncertainties," Reliab. Eng. Syst. Saf., **96**(9), pp. 965–975.
[32] Oberkampf, W. L., Trucano, T. G., and Hirsch, C., 2004, "Verification, Validation, and Predictive Capability in Computational Engineering and Physics," Appl. Mech. Rev., **57**(5), pp. 345–384.
[33] Wallstrom, T. C., 2011, "Quantification of Margins and Uncertainties: A Probabilistic Framework," Reliab. Eng. Syst. Saf., **96**(9), pp. 1053–1062.
[34] Kennedy, M. C., and Optagan, A., 2001, "Bayesian Calibration of Computer Models," J. R. Stat. Soc. B, **63**(3), pp. 425–464.
[35] Rebba, R., Mahadevan, S., and Huang, H., 2006, "Validation and Error Estimation of Computational Models," Reliab. Eng. Syst. Saf., **91**(10–11), pp. 1390–1397.
[36] Sankararaman, S., Ling, Y., and Mahadevan, S., 2011, "Uncertainty Quantification and Model Validation of Fatigue Crack Growth Prediction," Eng. Fract. Mech., **78**(7), pp. 1487–1504.
[37] Urbina, A., Mahadevan, S., and Paez, T., 2011, "Quantification of Margins and Uncertainties of Complex Systems in the Presence of Aleatoric and Epistemic Uncertainty," Reliab. Eng. Syst. Saf., **96**(9), pp. 1114–1125.
[38] Zhang, R., and Mahadevan, S., 2003, "Bayesian Methodology for Reliability Model Acceptance," Reliab. Eng. Syst. Saf., **80**(1), pp. 95–103.
[39] Chib, S., and Greenberg, E., 1995, "Understanding the Metropolis-Hastings Algorithm," Am. Stat., **49**(4), pp. 327–335.
[40] Salloum, M., Sargsyan,K., Jones, R., Debusschere, B., Najm, H. N., and Adalsteinsson, H., 2011, "Uncertainty Quantification in Multiscale Atomistic-Continuum Models," Uncertainty Quantification and Multiscale Materials Modeling Workshop, Santa Fe, NM, June 13–15.
[41] Rizzi, F., Jones, R. E., Debusschere, B., and Knio, O. M., 2013, "Uncertainty Quantification in MD Simulations of Concentration Driven Ionic Flow Through a Silica Nanopore: I. Sensitivity to Physical Parameters of the Pore," J. Chem. Phys., **138**(19), p. 194104.
[42] Rizzi, F., Jones, R. E., Debusschere, B., and Knio, O. M., 2013, "Uncertainty Quantification in MD Simulations of Concentration Driven Ionic Flow Through a Silica Nanopore: II. Uncertain Potential Parameters," J. Chem. Phys., **138**(19), p. 194105.
[43] Fishman, G., 1996, *Monte Carlo: Concepts, Algorithms, and Applications*, Springer–Verlag, New York.
[44] Giunta, A. A., Eldred, M., Swiler, L., Trucano, T., and Wotjkiewicz, S. J., 2004, "Perspectives on Optimization under Uncertainty: Algorithms and Applications," Proceedings of the 10th AIAA/ISSMO Multidisciplinary Analysis and Optimization Conference, Albany, New York.
[45] Cressie, N., 1991, *Statistics of Spatial Data*, John Wiley and Sons, New York.
[46] Xiu, D., and Karniadakis, G., 2002, "The Wiener-Askey Polynomial Chaos for Stochastic Differential Equations," SIAM J. Sci. Comput., **24**, pp. 619–644.
[47] Xiu, D., and Karniadakis, G., 2003, "A New Stochastic Approach to Transient Heat Conduction Modeling with Uncertainty," Int. J. Heat Mass Transfer, **46**, pp. 4681–4693.
[48] Xiu, D., 2009, "Fast Numerical Methods for Stochastic Computations: A Review," Commun. Comput. Phys., **5**, pp. 242–272.
[49] Xiu, D., and Hesthaven, J. S., 2005, "High Order Collocation Methods for Differential Equations with Random Inputs," SIAM J. Sci. Comput., **27**(3), pp. 1118–1139.
[50] Ghanem, R., and Spanos, P., 1991, *Stochastic Finite Elements: A Spectral Approach*, Springer-Verlag, New York.
[51] Ganapathysubramanian, B., and Zabaras, N., 2007, "Sparse Grid Collocation Schemes for Stochastic Natural Convection Problems," J. Comput. Phys., **225**, pp. 652–685.
[52] Smolyak, S., 1963, "Quadrature and Interpolation Formulas for Tensor Products of Certain Classes of Functions," Soviet Mathematics, Doklady, **4**, pp. 240–243.
[53] Najm, H. N., 2009, "Uncertainty Quantification and Polynomial Chaos Techniques in Computational Fluid Dynamics," Ann. Rev. Fluid Mech., **41**, pp. 35–52.
[54] Ma, X., and Zabaras, N., 2008, "An Adaptive Hierarchical Sparse Grid Collocation Algorithm for the Solution of Stochastic Differential Equations," J. Comput. Phys., **228**(8), pp. 3084–3113.
[55] Agarwal, N., and Aluru, N. R., 2010, "A Data-Driven Stochastic Collocation Approach for Uncertainty Quantification in MEMS," Int. J. Numer. Methods Eng., **83**(5), pp. 575–597.
[56] Stillinger, F. H., and Weber, T. A., 1985, "Computer Simulation of Local Order in Condensed Phases of Silicon," Phys. Rev. B, **31**(8), pp. 5262–5271.
[57] Plimpton, S., 1995, "Fast Parallel Algorithms for Short-Range Molecular Dynamics," J. Comput. Phys., **117**(1), pp. 1–19.
[58] Wang, Y. G., Qiu, B., McGaughey, A., Ruan, X. L., and Xu, X. F., 2013, "Mode-Wise Thermal Conductivity of Bismuth Telluride," J. Heat Transfer, **135**(9), p. 091102.
[59] Sun, L., and Murthy, J. Y., 2006, "Domain Size Effects in Molecular Dynamics Simulation of Phonon Transport in EDIP Silicon," Appl. Phys. Lett., **89**, p. 171919.
[60] Valleau, J. P., and Whittington, S. G., 1977, "A Guide to Monte Carlo for Statistical Mechanics," *Statistical Mechanics, Part A: Equilibrium Techniques*, B. J. Berne, ed., Plenum, New York.
[61] Patankar, S. V., 1980, *Numerical Heat Transfer and Fluid Flow*, Taylor & Francis, London.
[62] Purdue UQ Software, Available at http://memshub.org/site/memosa_docs/puq/